The EMBO Journal (2012) 31, 3363–3374 | © 2012 European Molecular Biology Organization | All Rights Reserved 0261-4189/12
www.embojournal.org

THE EMBO JOURNAL

Altered BCR signalling quality predisposes to autoimmune disease and a pre-diabetic state

Sebastian Königsberger[1], Jan Prodöhl[1], David Stegner[2], Vanessa Weis[1], Martin Andreas[1], Martin Stehling[3], Theresa Schumacher[1,4], Ruben Böhmer[1], Ina Thielmann[2], Judith MM van Eeuwijk[2], Bernhard Nieswandt[2] and Friedemann Kiefer[1,*]

[1]Mammalian Cell Signaling Laboratory, Department of Vascular Cell Biology, Max Planck Institute for Molecular Biomedicine, Münster, Germany, [2]DFG Research Center for Experimental Biomedicine, University Hospital and Rudolf Virchow Center, University of Würzburg, Würzburg, Germany and [3]Flow Cytometry Unit, Max Planck Institute for Molecular Biomedicine, Münster, Germany

The spleen tyrosine kinase family members Syk and Zap-70 are pivotal signal transducers downstream of antigen receptors and exhibit overlapping expression patterns at early lymphocytic developmental stages. To assess their differential kinase fitness *in vivo*, we generated mice, which carry a Zap-70 cDNA knock-in controlled by intrinsic Syk promoter elements that disrupts wild-type Syk expression. Kinase replacement severely compromised Erk1/2-mediated survival and proper selection of developing B cells at central and peripheral checkpoints, demonstrating critical dependence on BCR signalling quality. Furthermore, ITAM- and hemITAM-mediated activation of platelets and neutrophils was completely blunted, while surprisingly FcγR-mediated phagocytosis in macrophages was retained. The alteration in BCR signalling quality resulted in preferential development and survival of marginal zone B cells and prominent autoreactivity, causing the generation of anti-insulin antibodies and age-related glomerulonephritis. Development of concomitant fasting glucose intolerance in knock-in mice highlights aberrant B cell selection as a potential risk factor for type 1 diabetes, and suggests altered BCR signalling as a mechanism to cause biased cellular and Ig repertoire selection, ultimately contributing to B cell-mediated autoimmune predisposition.

The EMBO Journal (2012) **31,** 3363–3374. doi:10.1038/emboj.2012.169; Published online 22 June 2012
Subject Categories: signal transduction; immunology
Keywords: autoimmunity; B cell; Syk; Zap-70

*Corresponding author. Mammalian Cell Signaling Laboratory, Department of Vascular Cell Biology, Max Planck Institute for Molecular Biomedicine, Röntgenstrasse 20, Münster D-48149, Germany.
Tel.: +43 251 70365 230; Fax: +43 251 70365 297;
E-mail: fkiefer@gwdg.de
[4]Present address: Neurology Clinic and National Center for Tumor Diseases, Department of Neurooncology, University Hospital of Heidelberg, Heidelberg 69120, Germany.

Received: 31 January 2012; accepted: 18 May 2012; published online: 22 June 2012

Introduction

The early presence of autoantibodies in numerous autoimmune diseases like multiple sclerosis (Obermeier *et al*, 2008), systemic lupus erythematosus (Satoh *et al*, 2007) and type 1 diabetes (Bingley, 2010), as well as the success of B cell ablation strategies in alleviating autoimmune disease (Hu *et al*, 2007; Zekavat *et al*, 2008) put B cells at centre stage as participants in the onset of pathology. Both, B cell autoantibody production and autoantigen presentation could contribute to the detrimental priming of potentially self-reactive T cells, but the mechanisms of B cell miss-priming still await full clarification. Signal transduction through the B cell receptor (BCR) determines proper B lymphocyte development, selection and reactivity via discrete signalling thresholds. Hence, during the last years attention has been drawn to critical signalling components downstream of the BCR and their contribution to proper B cell selection. Signal mediators like, for example, the Src kinase family member Lyn acting through CD22 and SHP-1 (Somani *et al*, 2001; Hibbs *et al*, 2002; Ferry *et al*, 2005; Dubois *et al*, 2006), the Tec family kinase Btk (Middendorp *et al*, 2002; Kersseboom *et al*, 2006) and the negative regulatory protein tyrosine phosphatase Lyp (PTPN22) (Menard *et al*, 2011) have been associated with autoimmune phenotypes when either aberrantly expressed or mutated. As spleen tyrosine kinase family members have a central role in signal initiation downstream of antigen receptors, they might in terms of signalling quality serve as interesting candidates in the development of autoreactive B cells.

Whereas Zap-70, which is largely confined to T cells and NK cells (Chan *et al*, 1991), translates TCR- and integrin-mediated cues to the cell interior, Syk function predominates downstream of the BCR (DeFranco, 1987; Taniguchi *et al*, 1991), Fc receptors (Agarwal *et al*, 1993; Kolanus *et al*, 1993; Kiefer *et al*, 1998) and C-type lectins like, for example, Dectin-1 (Osorio and Reis e Sousa, 2011) and CLEC-2 (Kerrigan and Brown, 2010) in numerous haematopoietic cells. Interestingly, Zap-70 expression was recently reported to parallel, although at low amounts, Syk expression in developing murine bone marrow B cells (Fallah-Arani *et al*, 2008), and its presence is an essential prognostic marker for malignancy scoring of human B cell chronic lymphocytic leukaemia (Chen *et al*, 2002). Inferred from the reported crystal structure of Zap-70 (Deindl *et al*, 2007), Syk and Zap-70 likely adopt comparable autoinhibitory conformations and both kinases are allosterically activated through binding to phosphorylated ITAM (immunoreceptor tyrosine-based activation motif)-containing cytoplasmic receptor chains (Reth, 1989). Lack of Syk in murine thymocytes causes a partial arrest at the pre-TCR β-chain selection stage of T cell development (Palacios and Weiss, 2007), which suggests that differential kinase fitness was stringently adapted to the cellular and developmental contexts during B and T cell lymphocytic evolution. Syk is more readily activated by

autophosphorylation compared to Zap-70, which appears to rely on Src-family kinases for full activation, leading to the notion that Syk is a more active kinase compared to Zap-70 (Rolli *et al*, 2002). To assess general Syk-family kinase fitness *in vivo* in different cellular settings, we performed a kinase exchange expressing Zap-70 as a surrogate kinase of Syk. In particular, we wondered to which extent Zap-70 could functionally replace Syk.

In this study, we demonstrate that at comparable expression levels *in vivo*, Zap-70 acts as a hypoactive Syk surrogate downstream of ITAM-coupled immunoreceptors. Whereas the phagocytosis of B cell and Fcγ receptors is unaffected by the kinase exchange, platelet, macrophage and neutrophil activation as well as concomitant induction of effector functions, like platelet degranulation and neutrophil reactive oxygen intermediate production, are significantly blunted through the Zap-70 knock-in. In B cells, where BCR signalling quality has a major influence on developmental processes, the kinase exchange results in a failure of proper B cell selection that predisposes to B cell-mediated autoimmunity and likely increases the risk for type 1 diabetes development.

Results

Generation of $Syk^{Zap/Zap}$ knock-in mice

The partly redundant expression pattern of Syk-family kinases made us question to which extent Syk and Zap-70 exhibit interchangeable functions when physiologically expressed under the control of intrinsic Syk promoter elements. Therefore, we inserted a human pA-tailed Zap-70 cDNA (NM_001079) into the first coding exon of Syk (Supplementary Figure 1A-C), resulting in the disruption of endogenous Syk expression and a gene dosage-dependent increase in Zap-70 protein from $Syk^{+/+}$ over $Syk^{+/Zap\text{-}70}$ to $Syk^{Zap\text{-}70/Zap\text{-}70}$ (knock-in) mice (Supplementary Figure 1D). Of note, knock-in mice on a mixed C57/BL6 × 129/Sv genetic background were vital and fertile, with normal lifespan up to the time points where animals were sacrificed for experiments (⩽60 weeks). This allowed the analysis of differential kinase and concomitant cellular fitness of various compartments and at any age of interest. In addition, heterozygous $Syk^{+/Zap\text{-}70}$ littermates equipped with half the wild-type Syk dosage were phenotypically indistinguishable from $Syk^{+/+}$ mice and $Syk^{+/Zap\text{-}70}$ mice were therefore used as littermate controls (abbreviated Syk^{ctrl} or ctrl (figures)).

Syk kinase family exchange influences central B cell selection checkpoints

Analysis of Syk deficiency by adoptive transfer of $Syk^{-/-}$ fetal liver into irradiated hosts has previously demonstrated a complete arrest of bone marrow B cell development at the IgM^+ immature stage, whereas $Syk^{-/-}Zap\text{-}70^{-/-}$ double-deficient B cells do not develop beyond the pro- to pre-B transition (Cheng *et al*, 1995; Turner *et al*, 1995; Schweighoffer *et al*, 2003). Therefore, we analysed the capacity of Zap-70 to drive B cell development in our $Syk^{Zap\text{-}70/Zap\text{-}70}$ knock-in mice (abbreviated Syk^{ki} or ki (figures)) by multicolour flow cytometry following the Hardy classification scheme (Hardy *et al*, 1991). Syk^{ki} mice exhibited a significant reduction of fractions D–F (small pre-, immature, transitional B) compared to $Syk^{+/+}$ and $Syk^{+/Zap\text{-}70}$ mice (Figure 1A), which strongly affected total bone marrow cellularity, but left the myeloid ($Gr1^+$) compartment unaffected (Figure 1D, Supplementary Figure 2A). Essentially, B cell development partially arrested at the pre-BCR checkpoint (Figure 1B and E, fraction C) where pairing and surface expression of successfully rearranged IgH chains with a germline-encoded surrogate light chain (VpreB and λ5) triggers clonal pre-B cell expansion (Karasuyama *et al*, 1990). The differentiation block was not caused by aberrant pre-BCR surface expression as λ5 levels were comparable between Syk^{ctrl} and Syk^{ki} $B220^+CD43^+$ B cells (Figure 1F). In contrast to normal pre-BCR expression, forward scatter analysis of fraction A–C cells revealed a severe defect in pre-B blast formation (Figure 1G, right). This was further corroborated by cell cycle analysis, which showed that Zap-70 is largely inferior to Syk in driving pre-B cells into S/G2/M phase (Figure 1H and Supplementary Figure 2B). Recent work by Yasuda *et al* (2008) indicated that cell cycle entry of pre-B cells requires the activation of Erk1/2 through the pre-BCR. We therefore stimulated Syk^{ki} bone marrow B cells, consisting predominantly (∼85%) of early (fraction A–C) B cell stages, with anti-CD79b (Igβ) to mimic pre-BCR engagement and analysed pErk1/2 levels. Activation of Erk1/2 following CD79b ligation was severely compromised in Syk^{ki} mice (Figure 1I), in which only strongly reduced numbers of cells successfully traversed to the small pre-B cell stage (Figure 1C and E, fraction D). The reduced efficacy of passing the pre-BCR checkpoint was accompanied by an increase of early ($AnnexinV^+PI^-$) and late ($AnnexinV^+PI^+$) apoptotic cells in the IgM^- Syk^{ki} bone marrow compartment (Supplementary Figure 2C), which also includes apoptotic pre-B cells. Apoptosis rates of IgM^+ (immature/transitional) Syk^{ki} B cells were significantly elevated, which is likely explained by diminished prosurvival tonic BCR signalling (Supplementary Figure 2D). Apart from the pre-BCR/BCR signalling defects in Syk^{ki} mice, the developmental phenotype raised the question whether altered signalling quality through Zap-70 could potentially lead to an aberrant selection of a B cell pool prone to self reactivity.

Syk^{ki} mice exhibit an age-related accumulation of marginal zone B cells

Although the number of Syk^{ki} B cells successfully passing central development and populating the secondary lymphoid organs was significantly reduced (as exemplified by splenic $B220^+$ B cell counts, see Figure 2B), notably, Syk^{ki} mice generated $IgM^+IgD^{lo/-}$ transitional (T)1, IgM^+IgD^+ T2 and to a lesser extent $IgM^{lo/-}IgD^+$ mature B cells (Figure 2B). Despite the diminished B cell compartment, total splenocyte numbers (Supplementary Figure 3A) were largely replenished by an accumulation of $CD3^+CD4^+$ and $CD3^+CD8^+$ T cells in the splenic white pulp (Figure 2C). In 8- to 10-week-old mice, despite their absolute and equal increase, neither $CD3^+CD4^+$ nor $CD3^+CD8^+$ Syk^{ki} T cells showed signs of pre-activation as measured by CD69 expression (Supplementary Figure 3B). Also, the ratio of $CD3^+CD8^+CD44^{hi}CD62L^{lo}$ (effector/memory) versus $CD3^+CD8^+CD44^{lo}CD62L^{hi}$ (naive) Syk^{ki} T cells was comparable to Syk^{ctrl} ratios (Supplementary Figure 3D). Splenic $CD3^+CD4^+$ effector/memory T cell numbers of Syk^{ki} mice were increased to a lesser extent than their $CD3^+CD8^+CD44^{hi}CD62L^{lo}$ counterparts (Figure 2D), and the increase was counterbalanced by

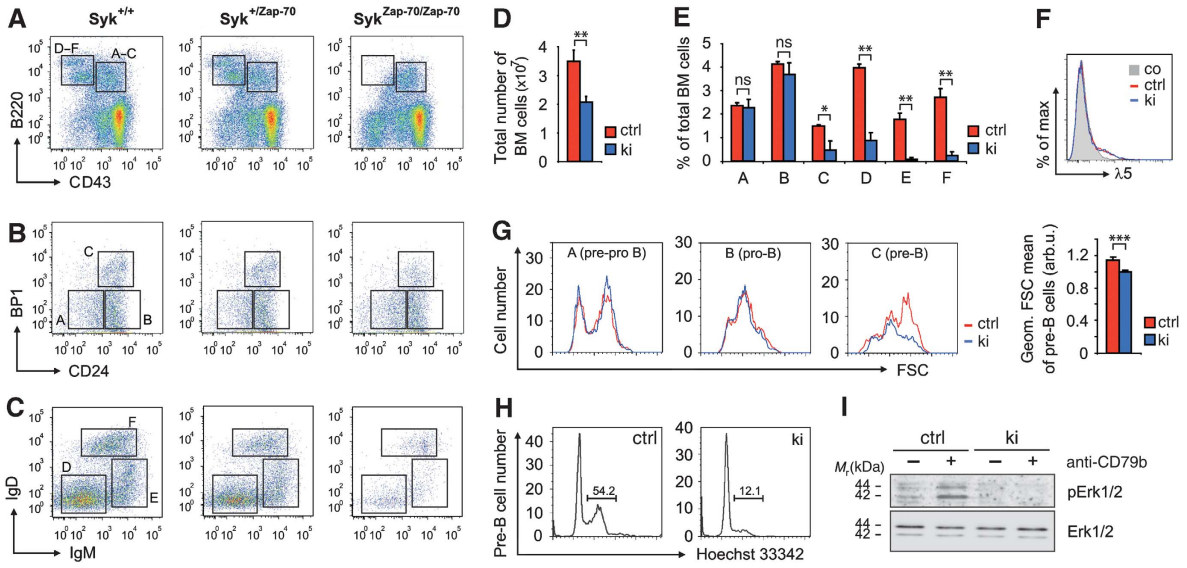

Figure 1 Attenuated pre-BCR-mediated prosurvival signalling through Erk1/2 affects central B cell selection. (**A–C**) Multicolour flow cytometric classification of $Syk^{+/+}$, $Syk^{+/Zap\text{-}70}$ (ctrl) and $Syk^{Zap\text{-}70/Zap\text{-}70}$ (ki) bone marrow B cell subsets according to the Hardy fractionation scheme (A = pre-pro, B = early pro, C = late pro/large pre, D = small pre, E = immature, F = transitional). (**D**) Total bone marrow cell numbers and (**E**) B cell subset statistics; the partial pro- to pre-B cell transition arrest significantly affected bone marrow cellularity. (**F**) λ5 expression on $B220^+CD43^+$ B cells indicated comparable pre-BCR levels between ctrl and ki cells. (**G**, left) Analysis of functional cell blast formation by assessment of the forward scatter (FSC) profiles of pre-pro, pro- and pre-B cells. (**G**, right) Pre-B cell forward scatter statistics. (**H**) DNA content-based (Hoechst 33342) cell cycle analysis of $B220^+CD43^+BP1^+CD24^+$ pre-B cells using five-colour flow cytometry; numbers indicate representative percentages of pre-B cells in S/G2/M phase. (**I**) Total p42/p44 (Erk1/2) and phospho-p42/p44 (pErk1/2) levels of bone marrow cells left untreated (−) or treated (+) with anti-CD79b (Igβ) for 2 min at 37°C. $^*P<0.05$, $^{**}P<0.01$, $^{***}P<0.001$; $n=8$ (**A–E**, **G**) and three (**F**, **H**, **I**) per group; error bars indicate means ± s.e.m. arb.u., arbitrary units; co, isotype control; Ig, immunoglobulin; ns, not significant. Figure source data can be found with the Supplementary data.

elevated $CD4^+CD25^+FoxP3^+$ nTreg cell numbers again resembling Syk^{ctrl} ratios (Figure 2E, Supplementary Figure 3C) which altogether indicated an accumulation of naive $CD3^+CD4^+$ T cells in the spleen. As adoptive transfer experiments had identified a unique function of Syk in promoting thymic T cell development at the DN3e stage (Palacios and Weiss, 2007), we wondered whether our kinase exchange would yield comparable results. Interestingly, Syk^{ki} thymic T cells exhibited a mild developmental arrest at the $CD4^-CD8^-CD44^-CD25^+$ DN3 stage (Supplementary Figure 4D and E), which however, did not affect single/double positive or total thymic T cell numbers (Supplementary Figure 4A-C). Recent studies (Siggs *et al*, 2007; Hsu *et al*, 2009) demonstrated that changing signalling quality through the TCR by hypomorphic Zap-70 alters the ratio of peripheral effector/memory versus naive T cells, affects nTreg numbers and predisposes to T cell-mediated autoimmunity. Our replacement of Syk by Zap-70 in thymocytes, however, had only a minor effect on the T cell compartment and resulted in a splenic white pulp 'fill up' by T cells balanced in subset ratios.

In contrast to the scarcely affected T cell populations, analysis of the B cell compartment revealed a rather unexpected pathogenesis apart from the severe B lymphopenia. Strikingly, Syk^{ki} mice accumulated $B220^+CD21^{hi}CD23^{lo/-}$ marginal zone (MZ) B cells from the age of 14 weeks onwards (Figure 2F and G), a phenomenon previously described for non-obese diabetic mice (Marino *et al*, 2008). MZ B cells constitute a population of likely transitional 2-derived, sessile and self-resplenishing cells with rarely somatically mutated mIg, harbouring carbohydrate and self-/poly-reactive specificities (Grey *et al*, 1982; Li *et al*, 2002). Syk^{ki} splenic B cells partially arrest at the T2 stage and seem to be preferentially selected towards the MZ fate (Figure 2A). This is indicated by the fact that Syk^{ki} MZ cells show a less severe reduction in cell number than the $B220^+CD21^{int}CD23^+$ follicular (FO)/T2 compartment which in ki mice is mainly composed of IgM^{high} T2 precursors (Figure 2F and G). Concomitantly, isotype-switched serum IgG titres were decreased while sIgM predominated in Syk^{ki} mice (Figure 2H). Taken together, our findings support the notion that BCR signalling quality is largely decisive to prime either towards the MZ or the FO B cell fate (Pillai and Cariappa, 2009).

Reduced Zap-70 kinase auto- and transphosphorylation activity result in diminished BCR-induced net-tyrosine phosphorylation, signal duration and Ca^{2+} flux

The differential requirements of Syk and Zap-70 to become fully activated and their substrate specificity have been under intense scrutiny since the first descriptions of the kinases about two decades ago (Chan *et al*, 1991; Taniguchi *et al*, 1991). A recent publication (Tsang *et al*, 2008) made use of a real-time fluorescence kinase assay to quantitatively characterize the molecular mechanisms of Syk and Zap-70 kinase activation *in vitro*. The kinetics of auto- and substrate phosphorylation were slower and the V_{max} was lower for Zap-70 compared to Syk. This finding supports the prevailing notion that Zap-70-mediated signalling indispensably relies on upstream Src-family kinase activity, while Syk can significantly contribute to its own activation and hence is more readily activated. To verify these findings, we stably expressed HA-tagged versions of a kinase-dead mutant

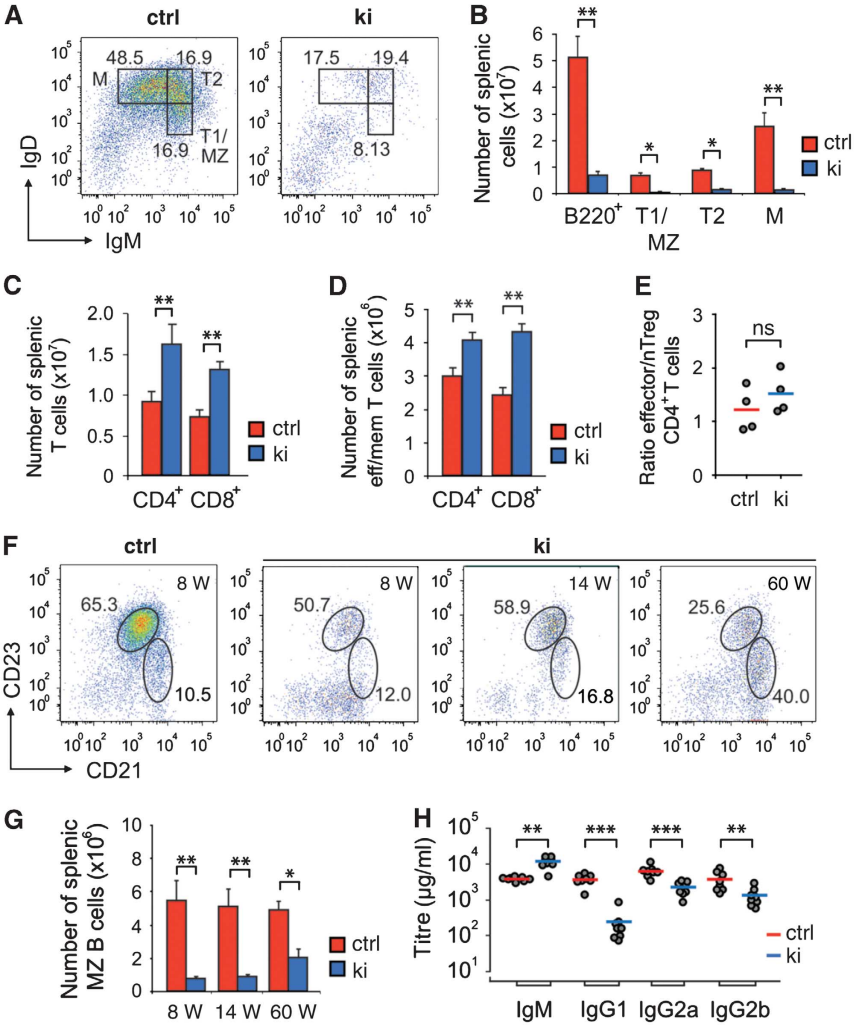

Figure 2 Age-related accumulation of *Syk*^{ki} marginal zone B cells. (**A**) B220$^+$ pre-gated splenic cells were stained with anti-IgM and anti-IgD to delineate transitional and mature B cell fractions. (**B**) Statistical analysis of total B220$^+$, transitional (T) 1/marginal zone (MZ), T2 and mature (M) splenic B cell and (**C**) CD4$^+$ and CD8$^+$ (CD3$^+$-pre-gated) T cell numbers in ctrl and ki mice. (**D**) Numbers of (CD3$^+$-pre-gated) CD44^{hi}CD62L^{lo} effector/memory CD4$^+$ and CD8$^+$ T cell subsets and (**E**) ratio of splenic CD4$^+$ effector/memory T versus CD4$^+$CD25$^+$ FoxP3$^+$ nTreg cells. (**F**, left) Representative dot plot of MZ (B220$^+$CD21^{hi}CD23$^{lo/-}$) and follicular (FO)/T2 (B220$^+$CD21^{int}CD23$^+$) B cells of ctrl mice at the age of 8 weeks (W); numbers in dot plots represent average percentages of B cell subsets. (**F**, right, **G**) Age-related accumulation of B220$^+$CD21^{hi}CD23$^{lo/-}$ MZ B cells in ki mice. (**H**) Pre-immune serum immunoglobulin (Ig) titres of ctrl and ki mice. For (**A**–**E**, **H**), mice were analysed at the age of 8–12 weeks. $^*P<0.05$, $^{**}P<0.01$, $^{***}P<0.001$; $n=7$ (**A**, **B**), 4 (**C**–**G**) and 8 (**H**) per group/age; error bars indicate means ± s.e.m. ctrl, control; M, mature; ns, not significant.

of Syk (HA:Syk [K402R]), wild-type Syk and Zap-70 in CHO cells (Figure 3A, left). We selected clones of equally low protein expression to avoid kinase pre-activation due to overexpression and determined the associated spontaneous kinase activity after HA-mediated immunoprecipitation. In line with earlier reports (Latour *et al*, 1996; Rolli *et al*, 2002), the mere presence of the allosteric activator Igβ sufficed to significantly activate Syk, while Zap-70 was inferior in *cis* but particularly in *trans* phosphorylation (Figure 3A, right). Anti-IgM-induced phosphorylation of Igβ was clearly weaker in primary *Syk*^{ki} splenic B cells as compared to *Syk*^{ctrl} B cells (Figure 3B) and in addition ITAM phosphorylation may have partly originated from Src kinase activity. Of note, precipitating Igβ from *Syk*^{ki} B cells yielded an additional band increasing in intensity with anti-IgM stimulation. Potentially, an increase in stimulation-dependent avidity of improperly self-restricted *Syk*^{ki} BCRs, co-precipitating under mild detergent conditions, resulted in autoantigen trapping. To assess the capacity of Zap-70 to transduce BCR-mediated signals, we stimulated sorted B220$^+$CD19$^+$ splenic B cells with anti-IgM F(ab′)2 and analysed net-phosphorylation kinetics by western blotting (Figure 3C). To further exclude the possibility that sorted B220$^+$CD19$^+$ ctrl B cells, which are largely composed of mature IgM^{lo}IgD^{hi} cells, would bias the comparison of *ex vivo* kinase activity, we additionally compared ctrl B220$^+$CD21^{hi}CD24^{hi} T2/MZ fraction B cells to ki B cells arresting mainly at the T2/MZ stage. In contrast to ctrl B cells, the Zap-70 knock-in generated a diminished BCR-induced net-phosphorylation response, resulting in faster off-signal kinetics. When we addressed anti-IgM-induced Ca^{2+} responses, *Syk*^{ki} BCRs only started to mobilize intracellular Ca^{2+} at high ligand concentrations, whereas the store-operated calcium entry (SOCE) into knock-in B cells was comparable to *Syk*^{ctrl} cells (Figure 3D), indicating that Syk kinase activity is indispensable for Ca^{2+} signal initiation but largely dispensable for SOCE response regulation.

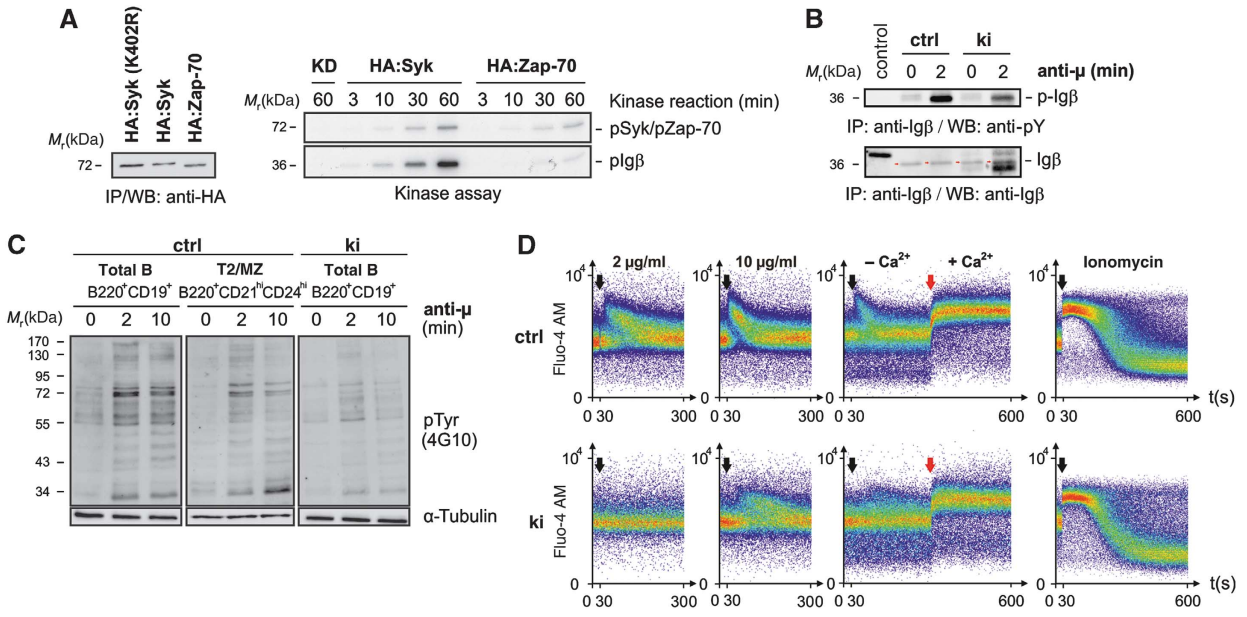

Figure 3 Reduced Syk-family kinase activity in Syk^{ki} cells translates into attenuated anti-IgM-induced phosphotyrosine signalling and a diminished B lymphocytic Ca^{2+} response. (**A**, left) To compare their auto- and transphosphorylation capacity, HA:Syk and HA:Zap-70 were stably expressed in CHO cells at comparable, low levels as shown by anti-HA immunoprecipitation (IP) and western blotting (WB). A kinase-dead mutant (KD) of Syk, HA:Syk(K402R) served as negative control. Associated kinase activity was assayed by incubation of a part of the anti-HA immunoprecipitated material *in vitro* in the presence of Mg^{2+}, γ-ATP-^{32}P and recombinant GST-Igβ (**A**, right) for the indicated time points. (**B**) To assess the phosphorylation state of Igβ *in vivo*, splenic B cells from Syk^{wt} and Syk^{ki} mice were left untreated (0) or stimulated with anti-IgM (anti-μ) for 2 min; subsequently, Igβ (red arrows) was immunoprecipitated and the amount of total Igβ and p-Igβ (4G10) was determined. (**C**) Phosphotyrosine levels (4G10) of total ctrl (B220$^+$CD19$^+$), T2/MZ ctrl (B220$^+$CD21^{hi}CD24^{hi}) and total ki (B220$^+$CD19$^+$) B cell lysates after anti-IgM F(ab′)2-mediated stimulation. (**D**) Reduced anti-IgM-induced calcium responses of fluo-4 AM-loaded splenic B220$^+$CD19$^+$ ki B cells; black arrows indicate the addition of anti-IgM at concentrations depicted above response curves; red arrows mark the addition of extracellular Ca^{2+} (1.5 mM) to measure the store-operated calcium entry after depleting ER stores with anti-IgM (10 μg/ml); ionomycin was used as a positive control. Each figure is representative for three independent experimental repeats; KD, kinase-dead. ctrl, control; Ig, immunoglobulin. Figure source data can be found with the Supplementary data.

Kinase exchange abrogates ITAM and hemITAM signalling in platelets

Apart from the reduced capacity of Zap-70 to properly regulate development and reactivity in B lymphocytes, we further assessed its function downstream of ITAM-coupled receptors in other haematopoietic cell populations, including platelets. Of note, basal blood parameters of Syk^{ki} mice, including red blood cell and platelet counts were comparable to Syk^{ctrl} mice (Supplementary Figure 5A). Furthermore, the surface expression of major glycoproteins and integrins was largely unchanged in Syk^{ki} platelets compared to controls (Supplementary Figure 5B) and Zap-70 expression was readily detected in Syk^{ki} platelets (Supplementary Figure 5C). This excluded a lack of kinase expression through decreased protein stability as a possible reason for observed differences in platelet activation. To delineate potential activation deficiencies, we stimulated isolated platelets with various agonists and assessed their activation by flow cytometry, measuring activated αIIbβ3-integrin by the use of the JON/A-PE antibody (Bergmeier *et al*, 2002; Figure 4A) and degranulation-dependent P-selectin exposure (Figure 4B). ADP, the TxA_2 analogue U46619 and thrombin all signal via G protein-coupled receptors (GPCRs), while CRP (collagen-related peptide) and the snake venom convulxin rely on GPVI/FcγR-mediated activation. Finally, rhodocytin binds and activates CLEC-2, a C-type lectin-like type II transmembrane receptor that signals through single YxxL hemi-ITAM motifs in a Syk-dependent manner (Fuller *et al*, 2007; May *et al*, 2009; Hughes *et al*, 2010). In Syk^{ki} platelets, αIIbβ3 activation and P-selectin upregulation remarkably failed to exceed resting state levels upon CRP, rhodocytin and convulxin stimulation. As αIIbβ3 is the main platelet integrin mediating adhesion, aggregation and spreading to the extracellular matrix upon vessel injury (Nieswandt *et al*, 2009), we investigated the potential of Syk^{ki} platelets to aggregate in response to GPCR (thrombin), GPVI (collagen, CRP) and CLEC-2 (rhodocytin) stimulation (Figure 4C). In line with the flow cytometric data, Syk^{ki} platelets failed to aggregate upon ITAM/hemITAM-coupled receptor triggering. The delayed and weak residual aggregation of Syk^{ki} platelets to collagen (Figure 4C, graph2) likely originated from integrin α2β1-mediated platelet attachment to the matrix protein followed by weak outside-in activation through the adhesion receptor. In contrast, no such response was observed upon CRP stimulation, which solely acts through GPVI. This altogether demonstrates that Zap-70 kinase is insufficient to sustain signalling downstream of ITAM- and hem-ITAM-coupled receptors in platelets.

Zap-70 kinase function suffices to trigger BCR- and FcγR-mediated endocytosis, but fails to replace Syk in effective ROS production upon immune complex-mediated stimulation in neutrophils

The failure of FcγR-mediated platelet activation in Syk^{ki} mice raised the question whether ITAM-coupled receptors retained any functionality in mononuclear phagocytes and granulocytes. We therefore derived macrophages from bone marrow cultures and assessed their ability to phagocytose either *E. coli* pHrodo particles (Figure 5A) or IgG-coated sheep red

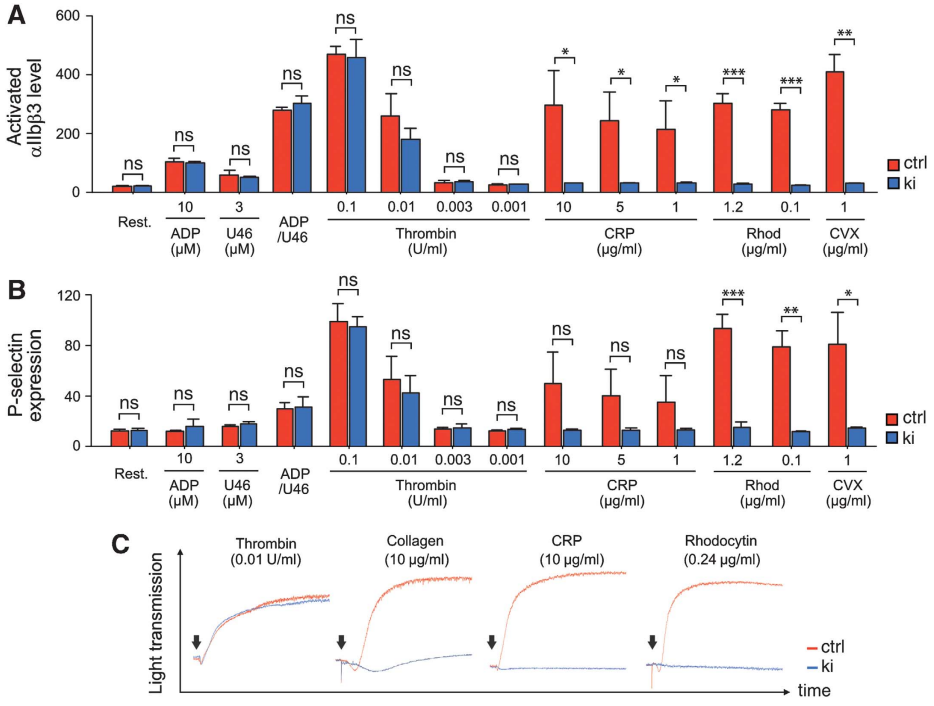

Figure 4 Impaired ITAM and hemITAM-coupled receptor signal transduction in Syk^{ki} platelets. After stimulation with the indicated agonists, platelet surface levels of activated αIIbβ3-integrin (JON/A-binding, **A**) and P-selectin (**B**) were measured by flow cytometry. Whereas GPCR-mediated signal transduction (ADP, U46619, thrombin) was comparable in ctrl and ki platelets, signalling via GPVI (CRP/convulxin) and CLEC-2 (rhodocytin) failed to activate αIIbβ3 or elicit Syk^{ki} platelet degranulation responses. (**C**) Platelet aggregometry revealed impaired aggregation of Syk^{ki} platelets in response to collagen, CRP and rhodocytin; arrows denote the addition of the agonists and each response curve covers 10 min of signal acquisition; $*P<0.05$, $**P<0.01$, $***P<0.001$. CRP, collagen-related peptide; ctrl, control; CVX, convulxin; ns, not significant; rhod, rhodocytin.

blood cells (SRBCs; Figure 5B) to discriminate ITAM-independent scavenger receptor- from ITAM-dependent FcγR-mediated phagocytosis. Overall, Syk^{ctrl} and Syk^{ki} macrophages showed comparable uptake kinetics in response to either stimulus, albeit FcγR-mediated SRBC uptake in knock-in macrophages was slightly delayed for the first 5 min (Figure 5B, right; $P=0.047$). Likewise, anti-IgM-induced BCR uptake kinetics were comparable between Syk^{ctrl} and Syk^{ki} splenic B220$^+$ B cells (Supplementary Figure 3B). These findings altogether indicated that Zap-70 can compensate for Syk in ITAM-coupled receptor internalization. Next, we isolated Syk^{ki} polymorphonuclear neutrophils and analysed their ability to produce reactive oxygen species (ROS) upon BSA–IgG-H_2DCF immune-complex-mediated FcγR triggering. Neutrophil uptake of *E. coli* pHrodo particles (Figure 5C) as well as the production of ROS upon bacterial tripeptide (fMLP) and PMA stimulation (Figure 5D, right) were indistinguishable between Syk^{ctrl} and Syk^{ki} mice, demonstrating that both responses were principally unaffected by the kinase exchange. However, upon immune complex (IC) addition, the generation of reactive oxygen intermediates was significantly reduced (Figure 5D, left), demonstrating that also in polymorphonuclear neutrophils the hypoactive surrogate kinase Zap-70 fails to compensate for essential Syk signalling functions downstream of FcγRs.

Syk^{ki} mice suffer from autoantibody immune complex-mediated glomerulonephritis and exhibit signs of a pre-diabetic state

On the basis of our observation that Zap-70 has a weaker, but still significant, ability to drive B cell development, we hypothesized that B cells with potentially autoreactive BCR specificities were likely to misinterpret, otherwise proapoptotic, bone marrow-derived BCR signals due to attenuated signal transduction. To test whether the antibodies produced by Syk^{ki} mice were properly self-restricted, we incubated human epithelial (Hep-) 2 cells with Syk^{ctrl} (Figure 6A, left image) or Syk^{ki} (Figure 6A, middle panel) sera and stained the cells with anti-IgM-FITC or anti-IgG-FITC. Strikingly, Syk^{ki} sera displayed prominent autoreactivity against cytoplasmic antigen (Figure 6A, right) but interestingly, never exhibited anti-nuclear staining. Autoreactive antibodies formed μ-type (Figure 6B, upper panel, right) and γ-type (Figure 6B, middle panel, right) IC deposits in Syk^{ki} kidneys, staining weakly for C3 (Figure 6B, lower panel, right) and eliciting age-related glomerulonephritis. PAS-stained paraffin sections of Syk^{ki} mice at the age of 60 weeks (Figure 6C, iii and iv) revealed that IC deposition strongly affected glomerular architecture, indicated by an increase of basement membrane, glomerular mesangial hypercellularity, mesangial matrix accumulation and an overall increase in Bowman capsule size (Figure 6D). Syk^{ki} mice at the age of 12 weeks also exhibited mild but significant proteinuria (Figure 6E). The extensive cytoplasmic Hep-2 cell staining of Syk^{ki} sera made us curious about the antigens recognized by Syk^{ki} autoantibodies. Therefore, we analysed Syk^{ki} serum reactivity towards dsDNA and insulin, two model antigens that are well-established targets in B cell co-mediated autoimmune disease. Intriguingly, sIgM of Syk^{ki} mice showed no significant increase in anti-dsDNA reactivity compared to Syk^{ctrl} sera, which correlated well with the lack of anti-nuclear Hep-2 staining (Figure 6F). However, Syk^{ki} sera highly reacted to

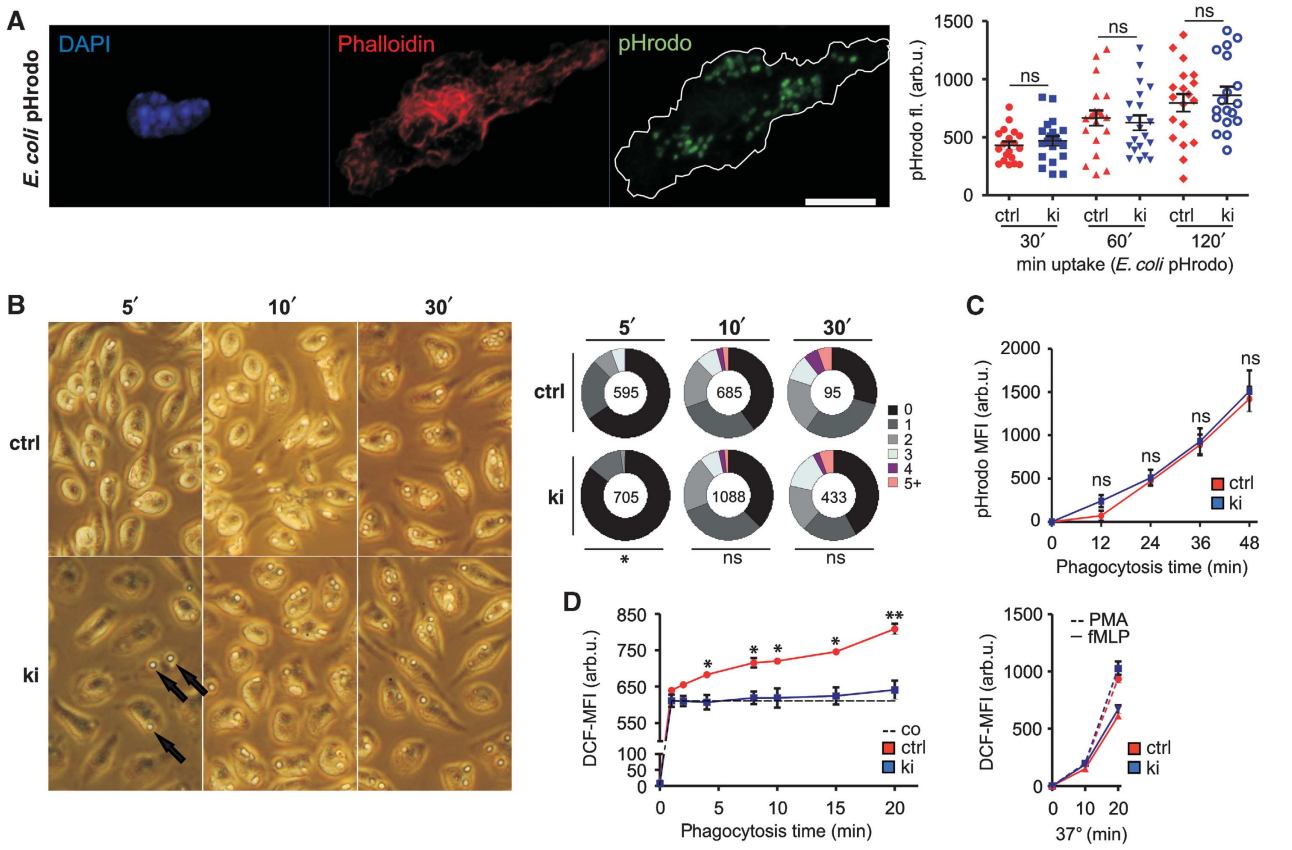

Figure 5 Differential requirements of Syk-family kinase activity for macrophage or polymorphonuclear neutrophil FcγR-mediated immune complex phagocytosis versus reactive oxygen species production. (**A**) Bone marrow-derived macrophages and (**C**) polymorphonuclear cells were incubated with *E. coli* particles to compare scavenger receptor-mediated uptake kinetics between ctrl and ki cells, delineating the functionality of non-ITAM-bearing receptors. (**A**, left) Representative image of a ctrl macrophage triple stained for the nucleus (4,6-diamidino-2-phenylindole, DAPI), F-actin (Phalloidin) and internalized pHrodo particles; scale bar = 10 μm. (**A**, right) Integrated pHrodo fluorescence determined within the F-actin$^+$ footprint of 20 macrophages for each condition 30, 60 and 120 min after particle addition. (**B**) To assess FcγR-mediated phagocytosis in macrophages, sheep erythrocytes (arrows) were opsonized with anti-hemolysin antibodies and incubated with macrophages for 5, 10 and 30 min at 37°C; pie charts indicate percentages of macrophages having internalized 0 to 5+ SRBCs, and numbers in the centre indicate the total number of macrophages analysed per condition. (**C**) Uptake of pHrodo *E. coli* particles by PMNs showed that proper Syk kinase activity was also dispensable for scavenger receptor-mediated phagocytosis in PMNs. (**D**, left) IgG-BSA-H_2DCF immune complex-induced ROS production was severely compromised in Syk^{ki} PMNs, whereas fMLP (10^{-6} M) and PMA (10^{-7} M) elicited comparable responses (**D**, right), indicating selective ablation of FcγR-mediated signalling. $^*P<0.05$, $^{**}P<0.01$; $n=3$ (**B**–**D**). arb.u., arbitrary units; co, control (on ice); ctrl, control; DCF, dichlorofluorescein; ns, not significant; PMA, phorbol-12-myristate-13-acetate.

recombinant insulin (Figure 6G), which could reflect a failure during negative selection of Syk^{ki} B cells towards soluble rather than particulate antigens. Following overnight starvation, already at the age of 14 weeks, Syk^{ki} mice showed significantly increased levels of fasting blood glucose (Figure 6H), one of the early hallmarks in the onset of type 1 diabetes. Intraperitoneal injection of D-glucose, however, resulted in comparable kinetics of blood glucose reduction in Syk^{ctrl} and Syk^{ki} mice (Figure 6I), confirming the pre-diabetic state. We additionally determined serum C-peptide, C3, C4, creatinine and BUN levels of 14-week-old ctrl and ki mice (Supplementary Figure 6A-E). The absence of overt inflammatory indicators and pancreatic infiltration (Supplementary Figure 6F) argues at least in young mice against severe renal damage and systemic complement activation. B cell autoantibody production and possible cognate feedback function for diabetogenic T cells may be counteracted by defects in IC and FcγR receptor-mediated activation of Syk^{ki} APCs, however, this compensatory mechanism may be lost with increasing age.

To further quantitate insulin-reactive clones within the Syk^{ki} B cell pool, we performed Elispot assays on sorted splenic B220$^+$CD19$^+$ B cells, which yielded, in contrast to the non-reactive wild-type controls, IgM reactivities towards insulin at a frequency of roughly 0.08% (Figure 6J, right). On a systemic level, bacterial antigens have been suggested to rather protect from type 1 diabetes due to a shift towards T_H2-mediated immunity (Sadelain *et al*, 1990; Lee *et al*, 2004). In our model system of aberrantly selected B cells, *ex vivo* stimulation with lipopolysaccharide increased the amount of anti-insulin autoantibody production, as indicated by IgM spot enlargement (Figure 6J, left). This finding, together with the recently reported splenic MZ helper response of neutrophils following LPS-mediated priming of macrophages and sinusoidal endothelial cells (Puga *et al*, 2011), provokes the question whether the unfavourable combination of danger signals and autoantigenic responses by self-reactive BCRs might foster the survival of autoreactive clones, resulting in an increased likelihood of antigenic presentation to T cells.

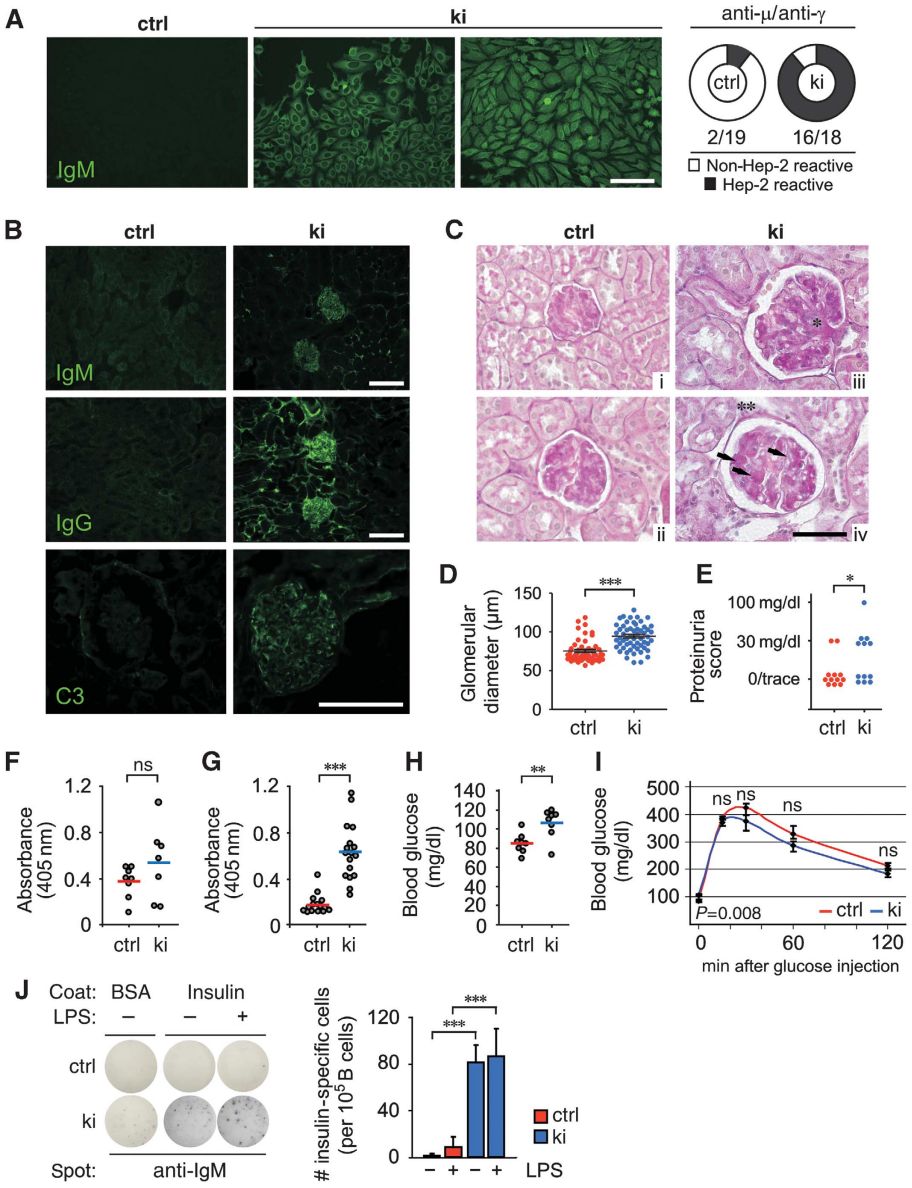

Figure 6 Syk^{ki} mice produce anti-insulin autoantibodies and develop age-related glomerulonephritis. (**A**) Permeabilized Hep-2 cells were incubated with Syk^{ctrl} or Syk^{ki} mouse sera, stained with anti-IgM-FITC or anti-IgG-FITC and analysed for Hep-2 reactivity via epifluorescence microscopy (Zeiss Axioscope, ×10, scale bar = 30 μm). (**A**, left image and middle panel) Representative images indicating prominent cytoplasmic Hep-2 reactivity (IgM depicted) of ki sera. (**A**, right) Numbers below pie charts indicate Hep-2 reactive sera (IgM^+ and IgG^+)/total number of animals analysed. (**B**) Kidney cryosections of ctrl and ki mice (8 weeks) were stained with anti-IgM-FITC (upper panel), anti-IgG-FITC (lower panel) and anti-C3 to assess glomerular immune complex and complement deposition (×20/×63, scale bar = 100 μm). (**C**) Periodic acid Schiff staining of kidney paraffin sections from Syk^{ctrl} (i, ii) and Syk^{ki} (iii, iv) mice at the age of 60 weeks (×63, scale bar = 50 μm) showed significant Syk^{ki} glomerular mesangial hypercellularity (*), mesangial matrix accumulation (arrows) and basement membrane increase (**). (**D**) Quantification of glomerular diameter and (**E**) proteinuria in Syk^{ctrl} and Syk^{ki} mice. (**F**) dsDNA-specific IgM titres were comparable between Syk^{ctrl} and Syk^{ki} mice, while (**G**) insulin-specific IgM titres were elevated in ki mice (8–12 weeks). (**H**) Basal blood glucose levels of 14-week-old Syk^{ctrl} and Syk^{ki} mice were measured after 16 h of chow starvation and (**I**) 0, 15, 30, 60 and 120 min after intraperitoneal injection of D-glucose (2 g/kg). (**J**) To test whether the anti-insulin-specific IgM titres in Syk^{ki} mice were aggravated upon TLR-4 stimulation of MZ B cells, sorted $B220^+CD19^+$ splenic B cells were incubated with LPS for 36 h and analysed for spot enlargement upon stimulation. $^*P<0.01$, $^{**}P<0.01$, $^{***}P<0.001$; $n = 18/19$ (**A**), 3 per age (**B**, **C**), 4 (**D**, ~100 glomeruli total), 12 (**E**), 8 (**F**), 18 (**G**), 8 (**H**, **I**) and 3 (**J**) per group; error bars indicate means ± s.e.m. BSA, bovine serum albumin; ctrl, control; Ig, immunoglobulin; LPS, lipopolysaccharide; ns, not significant.

Discussion

The non-receptor protein tyrosine kinases Syk and Zap-70 are indispensable signalling mediators in haematopoietic cells. The fact that throughout development, B cells co-express low levels of Zap-70 (Fallah-Arani *et al*, 2008) and thymic T cells start out with Syk expression being gradually replaced by Zap-70 (Palacios and Weiss, 2007) raised to us the question of functional kinase redundancy *in vivo*. In this manuscript, we demonstrate that replacement of Syk by Zap-70 causes differential cellular response fitness in mice. While, except for FcγR-mediated phagocytosis, ITAM- and hemITAM-coupled effector pathways requiring immediate and robust signalling responses were virtually abolished in myeloid cells, Zap-70 had the potential to sustain a certain degree of signalling

downstream of BCRs. This allowed B cells to preferentially survive in the pool of MZ B cells, caused significant serum autoreactivity due to aberrant cellular selection and hence, increased the risk for autoimmune disease.

During development, lymphocytes encounter a first major checkpoint, which probes for successful rearrangement and surface expression of the IgH or TCRβ chain by testing signalling through the pre-BCR and pre-TCR. Through the analysis of single and compound knockout mice, it has become clear that Syk and Zap-70 fulfil partially redundant functions downstream of these pre-antigen receptors. In T cells, Syk and Zap-70 both efficiently transduce pre-TCR signals and can largely replace each other. In mice deficient for either kinase, DP thymocytes are formed normally, while in double-deficient mice DP thymocyte formation is blocked (Cheng *et al*, 1997). Elegant competitive transplantation experiments revealed, however, that Syk specifically confers increased functional fitness during β-chain selection (Palacios and Weiss, 2007), allowing efficient transition from the DN3 to the DN4 stage. In pro-B cells, Syk is already superior to low levels of Zap-70 in supporting the pre-BCR-dependent pro- to pre-B cell transition. Consequently, Syk-deficient B cells display a partial block at this stage (Cheng *et al*, 1995; Turner *et al*, 1995). Double-deficient pro-B cells lacking Syk and Zap-70 are completely blocked at the pro- to pre-B cell transition (Schweighoffer *et al*, 2003). Retroviral rescue of $Syk^{-/-}$ fetal liver cells with either kinase showed that Zap-70 incompletely re-establishes B cell maturation capacity (Fallah-Arani *et al*, 2008). Our analyses of B cell development in the bone marrow of Syk^{ki} mice surprisingly showed that significant numbers of Syk^{ki} B cells developed beyond central pre-BCR and negative selection checkpoints. This development beyond the pre-BCR checkpoint is unlikely to be mechanistically explained by IL-7R-mediated rescue at the pro- to pre-B cell transition as the afore-mentioned $Syk^{-/-}Zap\text{-}70^{-/-}$ double knockout bone marrow cells completely fail to generate pre-B cells in reconstitution experiments (Schweighoffer *et al*, 2003). It rather suggests that an increase in Zap-70 expression, when driven by the Syk promoter, allows sufficient pre-BCR signalling, adding to the evidence that suggests functional complementation at the pre-BCR level. Syk^{ki} B cells, although prone to higher apoptosis rates likely due to diminished BCR-mediated pErk1/2 prosurvival signals, successfully populated secondary lymphoid organs and organized into small B cell FO areas adjacent to enlarged T cell zones (data not shown). The improved capacity of Syk^{ki} over $Syk^{-/-}$ B cells to pass the pre-B cell checkpoint and to differentiate into mature B cells may primarily be a consequence of the largely elevated expression of Zap-70 under the Syk promotor, providing enhanced kinase activity. Enzymatically, Syk is the more active kinase and depends to a lesser degree on upstream activation by Src kinases compared to Zap-70 (Kolanus *et al*, 1993; Latour *et al*, 1996). In line with these findings, Syk^{ki} BCRs were inferior in their ability to elicit efficient phosphotyrosine and Ca^{2+} responses and Syk more efficiently phosphorylated ITAM motifs, which subsequently act as allosteric kinase activators. These properties may explain the reduced pro- to pre-B cell transition of Syk^{ki} compared to Syk^{ctrl} B cells.

Furthermore, the SH2 domains of Syk both form a complete phosphotyrosine binding pocket, making them independently functional. In contrast, the N-terminal SH2-domain of Zap-70 is only capable of phosphotyrosine binding after establishing extensive contact with the C-terminal SH2 (SH2-C) domain, as part of the phosphotyrosine binding pocket is structurally provided by the SH2-C domain. This structural constraint results in a high selectivity of Zap-70 for the TCR/CD3 complex, which likely provides a conformational basis for the complete absence of hemITAM- and many FcγR-mediated signalling processes in Syk^{ki} myeloid cells. Interestingly, receptor-dependent endocytosis pathways were completely preserved, which had previously been demonstrated to critically depend on Syk expression. Our novel findings indicate that the intracellular targets causing phagocytic responses are qualitatively different from those responsible for, e.g., ROS generation and integrin inside-out activation and possible differences could involve reactivity to a short burst of kinase activity rather than sustained and localized signalling.

A number of recent studies has highlighted Syk in autoimmunity-related disease, as deletion of Syk in neutrophils protects from autoimmune serum transfer arthritis in mice (Elliott *et al*, 2011), hyperreactive/overexpressed Syk contributes to T cell malfunction in systemic lupus erythematosus (Krishnan *et al*, 2008) and targeting of Syk in dendritic cells abrogates FcγR-mediated cross-priming of diabetogenic T cells in RIP-mOVA mice (Colonna *et al*, 2010). The implication of ITAM-coupled immunoreceptor signalling in autoimmune diseases has provoked efforts to pharmaceutically intervene with aberrant protein function as exemplified by the development of the pharmacological inhibitors fostamatinib/R788 (Pine *et al*, 2007) and PRT062607 (Flight, 2011) for the treatment of rheumatoid arthritis. While these studies aimed to interfere with the detrimental elevation of Syk-mediated signalling associated with a sustained inflammatory response, we here analyse an *in vivo* condition representing decreased Syk-family kinase signalling to assess the importance of Syk in the generation of properly selected lymphocytic pools and to determine potential disease correlates.

Surprisingly, Syk^{ki} mice were viable and as homozygotes fertile, which allowed us not only to access the cellular consequences of the kinase exchange in various cell types, but also to assess its biological consequences in the absence of confounding factors like lethal irradiation and bone marrow transplants. An interesting finding in our model was that Syk^{ki} B cells were preferentially selected and more readily survived within the pool of splenic MZ B cells. Earlier publications reported that after substantial reduction of autoreactive potential during positive (Keenan *et al*, 2008) and essentially negative (Wardemann *et al*, 2003) central selection, the $IgM^{+}IgD^{+}$ T2 stage checkpoint of peripheral B cell development is decisive for FO versus MZ fate decision (Pillai and Cariappa, 2009). An alternative reason for the preferential selection/survival of MZ B cells in our model could be a preferential MZ fill up caused by lymphopenia, a phenomenon described for several BCR transgenic lines. In general, MZ B cells were reported to harbour autoreactive specificities and as they are potent activators of T cells due to a pre-activated phenotype must be properly excluded from follicles (Ekland *et al*, 2004). On

the basis of age-related accumulation of Syk^{ki} MZ B cells, we set out to test the idea of B cell autoreactivity caused by aberrant BCR-mediated selection through the hypoactive Syk-family member Zap-70. We found that Syk^{ki} B cells indeed turned out to specifically react to soluble self-antigens exemplified by high anti-insulin titres. The absence of anti-nuclear autoantibodies could be explained by various reasons: Either, negative central selection towards particulate self-antigens is still intact, inhibitory FcγRIIB co-ligation through ICs limits the expansion of high-affinity IgG-positive plasma cells or the Syk^{ki} germinal centre response is to some extent compromised in its ability to generate high-affinity antibodies. The later seems likely because it critically relies on the increase in BCR affinity and related signalling strength to compensate for decreasing antigenic availability. The autoreactive ICs deposited in Syk^{ki} kidneys staining brightly for IgG together with the fasting glucose intolerance of Syk^{ki} mice made us wonder why Syk^{ki} mice failed to develop more severe signs of autoimmune disease. Apart from the fact that, e.g., type 1 diabetes is a multifactorial disease requiring a combination of environmental factors and genetic susceptibilities (Redondo *et al*, 2001), the blunted reactivity of stimulating FcγRs in our mouse model system might explain the lack of progression to overt systemic autoimmune disease.

The basis for the very limited ability of Zap-70 to function downstream of B cell antigen receptors and stimulatory ITAM-coupled Fc receptors might be the differences in the way these receptors respond to discrete activation thresholds. FcR-mediated cellular activation acts through immune milieu (cytokine)-dependent co-expression of stimulatory and inhibitory receptors with common ligand binding properties (Nimmerjahn and Ravetch, 2006). FcRs provide immediate and robust signalling after reaching a critical ligand threshold making rather binary on/off signalling choices. In contrast, BCRs gradually respond to a broad spectrum of antigenic affinities reportedly allowing a certain degree of autoreactivity to avoid B cell repertoire leakiness. Therefore, we hypothesize that attenuated BCR-mediated signal transduction through hypoactive Syk, which may potentially be caused by mutation or loss of protein expression due to epigenetic alterations, allows for the positive selection of auto-/poly-reactive B cell clones and their survival through perpetuate receipt of autoantigenic stimulation. This might be an as yet unidentified risk factor contributing to autoimmune disease.

Materials and methods

Generation of $Syk^{Zap\text{-}70/Zap\text{-}70}$ knock-in mice

The Syk^{ki} targeting construct was created by fusing a polyA-tailed human Zap-70 cDNA (NM_001079) in frame with the (first coding) exon 2 ATG of a PAC clone (MRC geneservice UK, RPCI21-501)-derived genomic *Syk* sequence. Assembly of targeting construct was performed by modified Red/ET recombination, and a frt-flanked *Pgk* neomycin cassette was used for ES cell selection (Bohmer *et al*, 2010). DNA was transfected into R1 (129/Sv × 129/SvJ) ES cells and resulting colonies were analysed by Southern blotting (*Eco*RV digest; wt: 10.2 kb; ki: 9.5 kb). Neomycin cassette removal (Δ) was accomplished by crossing with transgenic *Pgk*-FLPe mice and verified by PCR. Injection of ES cells into C57BL/6 blastocysts resulted in chimeric mice that were backcrossed with the C57BL/6 background to establish the Syk^{ki} line. All animal experiments were approved by the Animal Experimentation Committee of the county of Münster and the Federal Ministry of Nature, Environment and Consumer Protection, North Rhine Westphalia.

Antibodies, flow cytometry and B lymphocyte cell cycle analysis

The following antibodies were used in the study: anti-mouse CD3 (145-2C11), CD4 (L3T4), CD8 (53-6.7), CD16/32 (2.4G2), CD19 (1D3), CD21/35 (7G6), CD23 (B3B4), CD25 (3C7), CD43 (S7), CD62L (MEL-14), CD69 (H1.2F3), CD79b (HM79b), CD179/λ5 (LM34), B220 (RA3-6B2), BP1, Gr1 (RB6-8C5) and IgM (R6-60.2), all from BD; CD24 (M1/69), CD44 (IM7) and FoxP3 (FJK-16s), all from eBioscience; IgM $F(ab')_2$ (Jackson), IgD (11-26c), IgG1, IgG2a and IgG2b, all from Southern Biotech; Syk (N-19), HA (F-7), CD79b (HM-79-12, AT107-2) and C3 (11H9), all from Santa Cruz; pY (4G10, Millipore), Zap-70 (99F2), Erk1/2 and pErk1/2, all from Cell Signaling Technology; HA (ab9134, Abcam); α-tubulin (B-5-1-2, Sigma); GPIb (Xia.G5), GPV (Gon.C2), GPIX (Xia.B4), GPVI (JAQ1), αIIbβ3 (JON/A), β3 (Luc.H11), β1 (BD), α2 (Sam.G4), α5 (Tap.A12) and CD9 (Nyn.H3), all from Emfret. The anti-CLEC-2 antibody has been described before (May *et al*, 2009). For flow cytometric analysis, preparations of spleen, thymus and flushes of bone marrow (femur and tibia) were blocked in PBS/3% FCS with anti-CD16/32 prior to staining with the indicated antibodies. Cell cycle analysis of B cells was performed by incubating cells for 1 h at 37°C with Hoechst 33342 (5 μg/ml) prior to staining with additional markers. Samples were acquired on a BD FACSAria II equipped with three lasers (blue: 488-nm solid state; red: 633-nm HeNe; violet: 405-nm solid state) and data were analysed using FlowJo software (v9.3.2., Treestar).

B cell stimulation, immunoprecipitation and western blotting

Sorted $B220^+CD19^+$ splenic B cells (purity ⩾98%) or bone marrow cells were stimulated with anti-CD79b or anti-IgM $F(ab')_2$ (10 μg/ml each) for the indicated time points and for measurement of total Erk1/2 and pErk1/2 levels immediately lysed in reducing loading buffer (125 mM Tris–HCl (pH 6.8), 2% SDS, 10% glycerol, 1.5% dithiotreitol, 0.001% bromphenol blue) prior to boiling for 5 min at 95°C. For immunoprecipitation of HA–Syk, HA–Syk (K402R), HA–Zap-70 and Igbeta, stimulated samples were immediately lysed in RIPA buffer (1% Triton X-100, 150 mM NaCl, 10 mM Tris (pH 7.5), 400 μM EDTA, 0.1% sodium dodecyl sulphate, 0.5% deoxycholate, 10 mM $Na_4P_2O_7$, 400 μM Na_3VO_4, 10 mM NaF, supplemented with protease inhibitor tablets (Roche)), precleared with Pansorbin (Merck), incubated with anti-HA or anti-CD79b antibodies for 1 h at 4°C, precipitated with protein G sepharose, washed and boiled in reducing loading buffer. Equivalents of 2×10^5 cells/lane were separated by PAGE, blotted onto nitrocellulose, incubated with the indicated primary and secondary-HRP antibodies and developed with ECL substrate (Thermo).

Ca^{2+} flux measurement

Splenic cells were resuspended to a final concentration of 2×10^6/ml and loaded with the fluorescent Ca^{2+} indicator Fluo-4 AM (4 μM) for 30 min in the dark, RT, in HBSS (pH 7.4), 20 mM Hepes, 1.5 mM $CaCl_2$, 1 mM $MgCl_2$, 1% FCS, 1.5 mM probenecid and 0.05% Pluronic F-127; after washing and 30 min of de-esterification at RT, samples were preheated at 37°C for 15 min and stained with anti-B220-APC for the last 5 min of the preheating step; subsequently, cells were washed with prewarmed buffer and after 30 s baseline acquisition stimulated with anti-IgM antibody (2 or 10 μg/ml). For B cell SOCE response measurement, intracellular Ca^{2+} stores were depleted by stimulating cells with anti-IgM (10 μg/ml) in $Ca2^+$-free medium (+EGTA) for 5 min and subsequently stimulated with 1.5 mM $CaCl_2$ for additional 5 min; positive controls were measured by the addition of 1 μM ionomycin (Sigma) after baseline acquisition.

Macrophage generation and PMN preparation

Macrophages were generated by seeding 10^6/ml bone marrow cells in IMDM, 10% FCS, 10% L929 culture supernatant (rmM-CSF), 1% X63/0 culture supernatant (rmIL-3), 50 μM β-ME; after 2 days, non-adherent cells were transferred to new dishes and cultured in IMDM, 10% FCS, 10% L929 culture supernatant, 50 μM β-ME for additional 7 days until >95% of the culture stained positive for F4/80 and CD11b. For the preparation of polymorphonuclear neutrophils, flushes (HBSS, 25 mM Hepes, 10% FCS) of bone marrow were pelleted, resuspended in HBSS, 25 mM Hepes and layered on Histopaque 1077/1119 density gradients for 30 min; after PMN layer isolation, cells were washed twice with HBSS/25 mM Hepes, counted and subjected to phagocytosis assays.

Phagocytosis assays

For the phagocytosis of IgG-opsonized SRBCs (IgG-SRBCs), 10^8 SRBCs (ACILA) were incubated in 1 ml HBSS (pH 7.4), 20 mM Hepes, 1.5 mM $CaCl_2$, 1 mM $MgCl_2$, 10 mM EDTA with an anti-hemolysin antibody (1:500, Sigma) for 1 h at 37°C, spun down, resuspended in ice-cold HBSS buffer and settled onto plated macrophages at a ratio of ~5:1. After 10 min of sedimentation on ice, unbound SRBCs were removed by washing five times with ice-cold PBS, and control samples were immediately fixed with 4% PFA and analysed for homogenous SRBC binding; to initiate phagocytosis, ice-cold PBS was replaced by prewarmed macrophage medium and incubated at 37°C for the indicated time points. To remove non-internalized SRBCs, macrophage medium was replaced by red cell lysis buffer (BD Pharmlyse) for 4 min at RT. Finally, SRBC lysis was stopped by the addition of macrophage medium, dishes were washed once with PBS and phase-contrast images were immediately taken on an inverted Nikon microscope (Eclipse TE2000-U) at ×10 magnification (NA = 0.30). Macrophage internalization of *E. coli* pHrodo particles (Invitrogen) was assessed by quantifying pHrodo signal intensity (z-stack (8/cell) maximum intensity projection) in relation to cell size (F-actin$^+$ area) of 20 cells per indicated time point with ImageJ; image acquisition was done on a Zeiss LSM-780 laser confocal scanning microscope at ×63 (NA = 1.40). *E. coli* pHrodo particle uptake by PMNs was analysed via flow cytometry and is presented as mean fluorescence intensity (MFI) of PE signal at the indicated time points. To analyse BCR uptake kinetics, total splenic cells were stained with anti-IgM-Biotin (Jackson, 10 μg/ml) prior to shifting cells to 37°C for the indicated time points; internalization was terminated by adding an excess of ice-cold PBS/3% FCS, followed by staining with Streptavidin-FITC (Jackson, 1:500) and anti-B220-APC (3 μg/ml) on ice. Cells were immediately analysed by flow cytometry, and FITC MFIs of B220$^+$ cells are displayed as % internalized receptor $[(-\mathrm{MFI_t}/\mathrm{MFI_{t0}} \times 100) + 100]$ at the indicated time points.

Statistical analysis

Data are presented as mean ± s.e.m. We analysed data using Student's *t*-test and Mann-Whitney rank-sum test as indicated in the figure legends (Sigma Plot 11.0).

Supplementary data

Supplementary data are available at *The EMBO Journal* Online (http://www.embojournal.org).

Acknowledgements

We thank Birgit Kempe for assistance in glucose tolerance assays, and Ludmila Kremer and Nannette Kümpel-Rink for in-house transgenic services; we thank Dietmar Vestweber for critically reviewing and discussing the manuscript. This work was supported in part by grants from the Deutsche Forschungsgemeinschaft (SFB 629) and the Max-Planck-Society to FK. JMMvE was supported by a grant of the *German Excellence Initiative* to the Graduate School of Life Sciences, University of Würzburg.

Author contributions: FK conceived the project; FK and SK designed and performed experiments, analysed and interpreted data and wrote the manuscript; RB and TS constructed the targeting vector and contributed to the generation and maintenance of the *Syk^{ki}* mouse line; JP, VW, MA, IT and JMMvE performed and analysed experiments; MS performed cell sorting; DS and BN designed and performed experiments, analysed data and contributed to the manuscript.

Conflict of interest

The authors declare that they have no conflict of interest.

References

Agarwal A, Salem P, Robbins KC (1993) Involvement of p72syk, a protein-tyrosine kinase, in Fc gamma receptor signaling. *J Biol Chem* **268:** 15900–15905

Bergmeier W, Schulte V, Brockhoff G, Bier U, Zirngibl H, Nieswandt B (2002) Flow cytometric detection of activated mouse integrin alphaIIbbeta3 with a novel monoclonal antibody. *Cytometry* **48:** 80–86

Bingley PJ (2010) Clinical applications of diabetes antibody testing. *J Clin Endocrinol Metab* **95:** 25–33

Bohmer R, Neuhaus B, Buhren S, Zhang D, Stehling M, Bock B, Kiefer F (2010) Regulation of developmental lymphangiogenesis by Syk(+) leukocytes. *Dev Cell* **18:** 437–449

Chan AC, Irving BA, Fraser JD, Weiss A (1991) The zeta chain is associated with a tyrosine kinase and upon T cell antigen receptor stimulation associates with ZAP-70, a 70-kDa tyrosine phosphoprotein. *Proc Natl Acad Sci USA* **88:** 9166–9170

Chen L, Widhopf G, Huynh L, Rassenti L, Rai KR, Weiss A, Kipps TJ (2002) Expression of ZAP-70 is associated with increased B-cell receptor signaling in chronic lymphocytic leukemia. *Blood* **100:** 4609–4614

Cheng AM, Negishi I, Anderson SJ, Chan AC, Bolen J, Loh DY, Pawson T (1997) The Syk and ZAP-70 SH2-containing tyrosine kinases are implicated in pre-T cell receptor signaling. *Proc Natl Acad Sci USA* **94:** 9797–9801

Cheng AM, Rowley B, Pao W, Hayday A, Bolen JB, Pawson T (1995) Syk tyrosine kinase required for mouse viability and B-cell development. *Nature* **378:** 303–306

Colonna L, Catalano G, Chew C, D'Agati V, Thomas JW, Wong FS, Schmitz J, Masuda ES, Reizis B, Tarakhovsky A, Clynes R (2010) Therapeutic targeting of Syk in autoimmune diabetes. *J Immunol* **185:** 1532–1543

DeFranco AL (1987) Molecular aspects of B-lymphocyte activation. *Annu Rev Cell Biol* **3:** 143–178

Deindl S, Kadlecek TA, Brdicka T, Cao X, Weiss A, Kuriyan J (2007) Structural basis for the inhibition of tyrosine kinase activity of ZAP-70. *Cell* **129:** 735–746

Dubois MJ, Bergeron S, Kim HJ, Dombrowski L, Perreault M, Fournes B, Faure R, Olivier M, Beauchemin N, Shulman GI, Siminovitch KA, Kim JK, Marette A (2006) The SHP-1 protein tyrosine phosphatase negatively modulates glucose homeostasis. *Nat Med* **12:** 549–556

Ekland EH, Forster R, Lipp M, Cyster JG (2004) Requirements for follicular exclusion and competitive elimination of autoantigen-binding B cells. *J Immunol* **172:** 4700–4708

Elliott ER, Van Ziffle JA, Scapini P, Sullivan BM, Locksley RM, Lowell CA (2011) Deletion of Syk in neutrophils prevents immune complex arthritis. *J Immunol* **187:** 4319–4330

Fallah-Arani F, Schweighoffer E, Vanes L, Tybulewicz VL (2008) Redundant role for Zap70 in B cell development and activation. *Eur J Immunol* **38:** 1721–1733

Ferry H, Crockford TL, Silver K, Rust N, Goodnow CC, Cornall RJ (2005) Analysis of Lyn/CD22 double-deficient B cells *in vivo* demonstrates Lyn- and CD22-independent pathways affecting BCR regulation and B cell survival. *Eur J Immunol* **35:** 3655–3663

Flight MH (2011) Deal watch: high hopes for oral SYK inhibitor in rheumatoid arthritis. *Nat Rev Drug Discov* **11:** 10

Fuller GL, Williams JA, Tomlinson MG, Eble JA, Hanna SL, Pohlmann S, Suzuki-Inoue K, Ozaki Y, Watson SP, Pearce AC (2007) The C-type lectin receptors CLEC-2 and Dectin-1, but not DC-SIGN, signal via a novel YXXL-dependent signaling cascade. *J Biol Chem* **282:** 12397–12409

Gray D, MacLennan IC, Bazin H, Khan M (1982) Migrant mu+ delta+ and static mu+ delta- B lymphocyte subsets. *Eur J Immunol* **12:** 564–569

Hardy RR, Carmack CE, Shinton SA, Kemp JD, Hayakawa K (1991) Resolution and characterization of pro-B and pre-pro-B cell stages in normal mouse bone marrow. *J Exp Med* **173:** 1213–1225

Hibbs ML, Harder KW, Armes J, Kountouri N, Quilici C, Casagranda F, Dunn AR, Tarlinton DM (2002) Sustained activation of Lyn tyrosine kinase *in vivo* leads to autoimmunity. *J Exp Med* **196:** 1593–1604

Hsu LY, Tan YX, Xiao Z, Malissen M, Weiss A (2009) A hypomorphic allele of ZAP-70 reveals a distinct thymic threshold for autoimmune disease versus autoimmune reactivity. *J Exp Med* **206:** 2527–2541

Hu CY, Rodriguez-Pinto D, Du W, Ahuja A, Henegariu O, Wong FS, Shlomchik MJ, Wen L (2007) Treatment with CD20-specific antibody prevents and reverses autoimmune diabetes in mice. *J Clin Invest* **117:** 3857–3867

Hughes CE, Pollitt AY, Mori J, Eble JA, Tomlinson MG, Hartwig JH, O'Callaghan CA, Futterer K, Watson SP (2010) CLEC-2 activates Syk through dimerization. *Blood* **115:** 2947–2955

Karasuyama H, Kudo A, Melchers F (1990) The proteins encoded by the VpreB and lambda 5 pre-B cell-specific genes can associate with each other and with mu heavy chain. *J Exp Med* **172:** 969–972

Keenan RA, De RA, Corleis B, Hepburn L, Licence S, Winkler TH, Martensson IL (2008) Censoring of autoreactive B cell development by the pre-B cell receptor. *Science* **321:** 696–699

Kerrigan AM, Brown GD (2010) Syk-coupled C-type lectin receptors that mediate cellular activation via single tyrosine based activation motifs. *Immunol Rev* **234:** 335–352

Kersseboom R, Ta VB, Zijlstra AJ, Middendorp S, Jumaa H, van Loo PF, Hendriks RW (2006) Bruton's tyrosine kinase and SLP-65 regulate pre-B cell differentiation and the induction of Ig light chain gene rearrangement. *J Immunol* **176:** 4543–4552

Kiefer F, Brumell J, Al-Alawi N, Latour S, Cheng A, Veillette A, Grinstein S, Pawson T (1998) The Syk protein tyrosine kinase is essential for Fcgamma receptor signaling in macrophages and neutrophils. *Mol Cell Biol* **18:** 4209–4220

Kolanus W, Romeo C, Seed B (1993) T cell activation by clustered tyrosine kinases. *Cell* **74:** 171–183

Krishnan S, Juang YT, Chowdhury B, Magilavy A, Fisher CU, Nguyen H, Nambiar MP, Kyttaris V, Weinstein A, Bahjat R, Pine P, Rus V, Tsokos GC (2008) Differential expression and molecular associations of Syk in systemic lupus erythematosus T cells. *J Immunol* **181:** 8145–8152

Latour S, Chow LM, Veillette A (1996) Differential intrinsic enzymatic activity of Syk and Zap-70 protein-tyrosine kinases. *J Biol Chem* **271:** 22782–22790

Lee IF, Qin H, Trudeau J, Dutz J, Tan R (2004) Regulation of autoimmune diabetes by complete Freund's adjuvant is mediated by NK cells. *J Immunol* **172:** 937–942

Li Y, Li H, Weigert M (2002) Autoreactive B cells in the marginal zone that express dual receptors. *J Exp Med* **195:** 181–188

Marino E, Batten M, Groom J, Walters S, Liuwantara D, Mackay F, Grey ST (2008) Marginal-zone B-cells of nonobese diabetic mice expand with diabetes onset, invade the pancreatic lymph nodes, and present autoantigen to diabetogenic T-cells. *Diabetes* **57:** 395–404

May F, Hagedorn I, Pleines I, Bender M, Vogtle T, Eble J, Elvers M, Nieswandt B (2009) CLEC-2 is an essential platelet-activating receptor in hemostasis and thrombosis. *Blood* **114:** 3464–3472

Menard L, Saadoun D, Isnardi I, Ng YS, Meyers G, Massad C, Price C, Abraham C, Motaghedi R, Buckner JH, Gregersen PK, Meffre E (2011) The PTPN22 allele encoding an R620W variant interferes with the removal of developing autoreactive B cells in humans. *J Clin Invest* **121:** 3635–3644

Middendorp S, Dingjan GM, Hendriks RW (2002) Impaired precursor B cell differentiation in Bruton's tyrosine kinase-deficient mice. *J Immunol* **168:** 2695–2703

Nieswandt B, Varga-Szabo D, Elvers M (2009) Integrins in platelet activation. *J Thromb Haemost* **7**(Suppl 1): 206–209

Nimmerjahn F, Ravetch JV (2006) Fcgamma receptors: old friends and new family members. *Immunity* **24:** 19–28

Obermeier B, Mentele R, Malotka J, Kellermann J, Kumpfel T, Wekerle H, Lottspeich F, Hohlfeld R, Dornmair K (2008) Matching of oligoclonal immunoglobulin transcriptomes and proteomes of cerebrospinal fluid in multiple sclerosis. *Nat Med* **14:** 688–693

Osorio F, Reis e Sousa C (2011) Myeloid C-type lectin receptors in pathogen recognition and host defense. *Immunity* **34:** 651–664

Palacios EH, Weiss A (2007) Distinct roles for Syk and ZAP-70 during early thymocyte development. *J Exp Med* **204:** 1703–1715

Pillai S, Cariappa A (2009) The follicular versus marginal zone B lymphocyte cell fate decision. *Nat Rev Immunol* **9:** 767–777

Pine PR, Chang B, Schoettler N, Banquerigo ML, Wang S, Lau A, Zhao F, Grossbard EB, Payan DG, Brahn E (2007) Inflammation and bone erosion are suppressed in models of rheumatoid arthritis following treatment with a novel Syk inhibitor. *Clin Immunol* **124:** 244–257

Puga I, Cols M, Barra CM, He B, Cassis L, Gentile M, Comerma L, Chorny A, Shan M, Xu W, Magri G, Knowles DM, Tam W, Chiu A, Bussel JB, Serrano S, Lorente JA, Bellosillo B, Lloreta J, Juanpere N *et al* (2011) B cell-helper neutrophils stimulate the diversification and production of immunoglobulin in the marginal zone of the spleen. *Nat Immunol* **13:** 170–180

Redondo MJ, Fain PR, Eisenbarth GS (2001) Genetics of type 1A diabetes. *Recent Prog Horm Res* **56:** 69–89

Reth M (1989) Antigen receptor tail clue. *Nature* **338:** 383–384

Rolli V, Gallwitz M, Wossning T, Flemming A, Schamel WW, Zurn C, Reth M (2002) Amplification of B cell antigen receptor signaling by a Syk/ITAM positive feedback loop. *Mol Cell* **10:** 1057–1069

Sadelain MW, Qin HY, Lauzon J, Singh B (1990) Prevention of type I diabetes in NOD mice by adjuvant immunotherapy. *Diabetes* **39:** 583–589

Satoh M, Chan EK, Sobel ES, Kimpel DL, Yamasaki Y, Narain S, Mansoor R, Reeves WH (2007) Clinical implication of autoantibodies in patients with systemic rheumatic diseases. *Expert Rev Clin Immunol* **3:** 721–738

Schweighoffer E, Vanes L, Mathiot A, Nakamura T, Tybulewicz VL (2003) Unexpected requirement for ZAP-70 in pre-B cell development and allelic exclusion. *Immunity* **18:** 523–533

Siggs OM, Miosge LA, Yates AL, Kucharska EM, Sheahan D, Brdicka T, Weiss A, Liston A, Goodnow CC (2007) Opposing functions of the T cell receptor kinase ZAP-70 in immunity and tolerance differentially titrate in response to nucleotide substitutions. *Immunity* **27:** 912–926

Somani AK, Yuen K, Xu F, Zhang J, Branch DR, Siminovitch KA (2001) The SH2 domain containing tyrosine phosphatase-1 down-regulates activation of Lyn and Lyn-induced tyrosine phosphorylation of the CD19 receptor in B cells. *J Biol Chem* **276:** 1938–1944

Taniguchi T, Kobayashi T, Kondo J, Takahashi K, Nakamura H, Suzuki J, Nagai K, Yamada T, Nakamura S, Yamamura H (1991) Molecular cloning of a porcine gene syk that encodes a 72-kDa protein-tyrosine kinase showing high susceptibility to proteolysis. *J Biol Chem* **266:** 15790–15796

Tsang E, Giannetti AM, Shaw D, Dinh M, Tse JK, Gandhi S, Ho H, Wang S, Papp E, Bradshaw JM (2008) Molecular mechanism of the Syk activation switch. *J Biol Chem* **283:** 32650–32659

Turner M, Mee PJ, Costello PS, Williams O, Price AA, Duddy LP, Furlong MT, Geahlen RL, Tybulewicz VL (1995) Perinatal lethality and blocked B-cell development in mice lacking the tyrosine kinase Syk. *Nature* **378:** 298–302

Wardemann H, Yurasov S, Schaefer A, Young JW, Meffre E, Nussenzweig MC (2003) Predominant autoantibody production by early human B cell precursors. *Science* **301:** 1374–1377

Yasuda T, Sanjo H, Pages G, Kawano Y, Karasuyama H, Pouyssegur J, Ogata M, Kurosaki T (2008) Erk kinases link pre-B cell receptor signaling to transcriptional events required for early B cell expansion. *Immunity* **28:** 499–508

Zekavat G, Rostami SY, Badkerhanian A, Parsons RF, Koeberlein B, Yu M, Ward CD, Migone TS, Yu L, Eisenbarth GS, Cancro MP, Naji A, Noorchashm H (2008) *In vivo* BLyS/BAFF neutralization ameliorates islet-directed autoimmunity in nonobese diabetic mice. *J Immunol* **181:** 8133–8144

